JOURNAL OF GEOPHYSICAL RESEARCH, VOL. 95, NO. D3, PAGES 2061–2072, FEBRUARY 28, 1990

In Search of Regularities in Extreme Rainstorms

EFI FOUFOULA-GEORGIOU

St. Anthony Falls Hydraulic Laboratory
Department of Civil and Mineral Engineering, University of Minnesota

LARRY L. WILSON

Department of Civil Engineering, University of Washington

Extreme rainstorms play an important role in the hydrologic design and operation of water resource systems. Due to the lack of complete knowledge of the complex meteorological mechanisms that produce and sustain extreme storms, statistical and correlation analyses are a valuable and complementary tool in identifying regularities of extreme rainfall characteristics. In this paper we have studied the statistical properties of several characteristics of extreme midwestern storms. In particular, we have analyzed the storm occurrence process in space and time, storm shape and orientation, total storm center depth, storm duration, storm areal extent, and depth-area relationships. Our analysis is based on the data base of extreme storms published by the U.S. Army Corps of Engineers. Several trends and regularities among extreme midwestern storms have been identified and are expected to prove useful in developing and/or evaluating empirical and physically based models of extreme rainfall.

INTRODUCTION

The description of the space-time characteristics of extreme storms is of vital importance to applied hydrology and water resources. It is usually these extreme events and the floods they produce that determine the design and operation of hydraulic structures, determine the shape of the land by the drastic geomorphic changes they induce, and often cause loss of property and sometimes life. Such extreme events are by definition infrequent and therefore more difficult to understand, observe, and model.

Perhaps the most important use of extreme storm models is in assessing the frequency of extreme floods. *Klemes* [1982] and *Eagleson* [1972] have long been advocates of a "causative approach" to estimation of extreme floods. They suggest that estimation of extreme floods and their probabilities should be based on a joint analysis of the causative factors involved, that is, extreme rainfall and catchment geomorphology, as opposed to a direct probabilistic analysis of streamflow records. Recent studies by *Eagleson* [1984] and *Eagleson and Wang* [1987] have stressed the importance of storm to catchment scales on the variability of the produced runoff. *Milly and Eagleson* [1988] have examined the effect of storm size on the rainfall-runoff relationship for cases where the storm size is comparable to the size of the modeled area. G. O. Tabios (unpublished manuscript, 1987) examined the effects of the storm orientation and speed on the streamflow hydrograph and concluded that these characteristics are important and should not be neglected in current design practices. *Alexander* [1963], *Gupta* [1972], and *Foufoula-Georgiou* [1989a] have studied a method for estimating the exceedance probability of extreme rainfall depths, using storm regionalization and transposition and taking into account the spatial rainfall structure and the storm/catchment interactions. Such studies require the statistical description of several storm characteristics, such as storm center depth, areal extent, storm duration, storm shape and orientation, and depth-area relationships. Also, the characterization of the occurrence process of extreme storms in space and time is an important element of any storm transposition or storm regionalization study.

Long records of the magnitude, location, and time of occurrence of extreme events, such as earthquakes, storms, floods, and droughts, do exist but are probably incomplete and not very accurate. Extreme storms have been recorded since 1819, and there exists a data base of a total of 853 storms in the contiguous United States. The data collection and processing was a joint effort of the U.S. Army Corps of Engineers and the U.S. Weather Bureau. From the 853 storms, 314 storms are either incomplete or the depth-area-duration (DAD) analysis is not considered very exact [*Shipe and Riedel*, 1976]. The most complete and accurate part of the data base is what is referred to as "storm rainfall." The storm rainfall data consist of 539 storms published in a report by the *U.S. Army Corps of Engineers* [1945–]. Each storm is described in two typical sheets including information such as the date of occurrence, total storm duration, storm location, total storm isohyetal maps, DAD tables for durations of 6, 12, 18, 24,... hours, and mass curves for selected stations. Additional supporting data are on file at the National Weather Service. This data base has been mainly used to derive estimates of probable maximum precipitation (PMP). With the exception of the study of *Boyer* [1957], these data have not been subjected to an extensive exploratory statistical analysis for the purpose of identifying regularities in the characteristics of extreme storms.

In this paper we present a statistical analysis of several characteristics of extreme midwestern storms. In particular, we have studied the extreme storm occurrence process in space and time, storm shape and orientation, total storm center depth, total storm duration, duration at the storm

Paper number 89JD01631.
0148-0227/90/89JD-01631$05.00

center, storm areal extent, and depth-area relationships. It is emphasized that our analysis is solely based on the data reported in the extreme storm catalog for the period 1891–1951 [*U.S. Army Corps of Engineers*, 1945–]. This storm catalog, due to its length and extensive areal coverage, provides a unique source of information about extreme storms. However, it should be realized that there are two main shortcomings associated with this data set. First, the data for each storm are possibly of different accuracy, since rain gage network density has considerably changed over time and is different from place to place [e.g., *Langbein and Hoyt*, 1959]. While it is clear that gage density does have an effect on the measured depths (e.g., see *Huff and Neill* [1957] for an empirical study and *Foufoula-Georgiou* [1989b] for a simplified mathematical approach to this problem), more research is needed before the statistical properties of the error can be quantified (as a function of storm parameters and rain gage density) and used for adjustment of the storm catalog depths. In the present analysis, it was assumed that all analyzed storms are of comparable accuracy. Another shortcoming of the storm catalog is that the reported data are of a nondetailed and processed form and do not permit an accurate estimation of some storm parameters, e.g., storm elongation, storm center duration. Thus for these parameters the results reported herein should be used only as indicative measures. Nevertheless, they establish the general trend and should prove useful in hydrologic modeling or simulation studies, where extreme storms are used for the estimation of design events.

DATA BASE OF EXTREME STORMS

The extreme storms used in our analysis are all of the catalog storms which have their centers, defined as the points with the maximum recorded depth, within the nine-state midwest area (North and South Dakota, Nebraska, Kansas, Minnesota, Iowa, Missouri, Wisconsin, and Illinois) and have a total 10 mi^2 (26 km^2) average depth greater than or equal to 9 inches (23 cm). It should be noted that the storm catalog does not report the maximum recorded depth as a point rainfall (d_o), but rather as the average depth over an area of 10 mi^2 around the storm center ($\bar{d}(10)$); $\bar{d}(10)$ is therefore used throughout this study as the representative storm center depth. The criteria given above provided us with a set of 77 storms for the period 1891–1951. These storms will be referred to hereafter as "extreme storms." They are listed in Table 1 together with their U.S. Army Corps of Engineers number and some other characteristics directly obtainable from the information given in the catalog. These characteristics are total storm duration, total 10 mi^2 average depth, maximum 24-hour 10 mi^2 average depth, areal extent and average depth within this area, storm location, and month and year of occurrence.

The selection of the cutoff level of 9 inches, although arbitrary, is believed to be low enough to provide us with a significant number of extreme storms and high enough to assure a complete storm sample, since the storm catalog may be incomplete with respect to less extreme storms. The storm catalog incompleteness cannot be easily assessed because the criteria used by the U.S. Army Corps of Engineers for including a storm in the catalog are not well defined and may have changed over the years. A partial assessment of the storm catalog incompleteness has been made herein via a frequency analysis of the storm center depths of all the midwest storms contained in the catalog for the period 1891–1951—a total of 170 storms (Figure 1). Assuming that the maximum recorded depths of all storms have comparable accuracy, this frequency analysis indicates that the number of catalog storms with total center depth less than 9 inches declines as the depth decreases. When viewed in a physical sense, this would not seem likely. If the records were complete for storms of all depths, one would expect to see more storms in the intervals of lower depths, since on the average, storms with smaller depths have a higher rate of occurrence. This analysis suggests that the storm catalog may not be complete with respect to storms of maximum depth less than 7 inches (18 cm) and it seems more likely to be complete with respect to storms of maximum depth greater than 9 inches. More definite conclusions may be reached from an analysis of daily rainfall data or discharge data, but such data-intensive tests have not been performed in this analysis, and the assumption has been made that the sample of 77 extreme storms is complete.

To get an idea of the magnitude and frequency of the 77 extreme storms studied, it is noted that their maximum 24-hour 10 mi^2 depth ranges between 5 and 22 inches (13 and 56 cm). Assuming uniform intensity and using the intensity-duration-frequency (IDF) curves of Iowa, most of these depths have return periods of well over 100 years (the 100-year maximum 24-hour depth is approximately 6 inches (15 cm)).

Because storm characteristics depend, in general, on the total storm depth and storm duration, it was found fruitful, for some of the analyses, to divide the set of 77 storms into two different groups: one group characterized by the 10 mi^2 average storm depth and the other by the total storm duration. Each of these groups was further subdivided in three subsets. The first group of subsets, based on the storm center depth, $\bar{d}(10)$, is

Set 1 (18 storms)

$$\bar{d}(10) \geq 13.0 \text{ inches (33 cm)}$$

Set 2 (26 storms)

$$10.5 \leq \bar{d}(10) < 13.0 \text{ inches}$$

Set 3 (33 storms)

$$9.0 \leq \bar{d}(10) < 10.5 \text{ inches (26.6 cm)}$$

The second group of subsets, based on the total storm duration, t_r, is

Set 4 (18 storms)

$$t_r \geq 120 \text{ hours}$$

Set 5 (31 storms)

$$78 \leq t_r < 120 \text{ hours}$$

Set 6 (28 storms)

$$10 \leq t_r < 78 \text{ hours}$$

SEASONAL AND CHRONOLOGICAL DISTRIBUTION OF STORMS

The seasonal distribution of all 77 storms is given in Figure 2. It is observed that most of the storms occur during the

TABLE 1. Characteristics of the Analyzed Storms Taken From the U. S. Army Corps of Engineers Catalog

U.S. Army Corps of Eng. Number	Duration, hours	Total 10 mi^2 Avg. Depth	Maximum 24-hr 10 mi^2 Avg. Depth	Areal Extent, mi^2	Storm Center Town	Storm Center State	Date
MR 4-24	54	21.7	21.7	63,000 (3.5)	near Boyden	IA	Sept. 17, 1926
MR 4-5	20	13.0	13.0	20,000 (3.5)	Grant Township	NE	June 03, 1940
MR 6-15	78	16.7	15.3	16,000 (4.6)	near Stanton	NE	June 10, 1944
MR 7-2A	78	19.4	15.0	45,000 (5.0)	near Cole Camp	MO	Aug. 12, 1946
MR 1-10	96	15.5	14.7	59,000 (4.4)	Woodburn	IA	Aug. 24, 1903
MR 2-29	78	13.9	12.2	113,500 (3.9)	Grant City	MO	July 09, 1922
MR 1-5	78	13.6	12.3	100,000 (3.9)	Primghar	IA	July 14, 1900
MR 10-2	108	18.2	8.6	57,000 (6.0)	nr Council Grove	KS	July 09, 1951
MR 8-20	120	16.9	11.5	50,000 (3.8)	near Holt	MO	June 18, 1947
MR 1-9	168	16.8	8.1	136,000 (4.8)	Abilene	KS	May 25, 1903
MR 3-14	120	14.6	8.8	120,000 (5.0)	Pleasonton	KS	Oct. 28, 1927
MR 4-2	96	12.8	12.8	30,000 (4.6)	Larrabee	IA	June 23, 1891
UMV 1-11	108	13.2	11.5	50,000 (4.8)	Ironwood	MI	July 18, 1909
UMV 2-9	120	13.1	6.5	57,100 (4.2)	Louisiana	MO	Aug. 10, 1916
UMV 2-18	180	13.0	8.1	70,000 (6.2)	Boonville	MO	Sept. 12, 1905
UMV 1-22	78	15.0	12.4	60,000 (4.7)	Hayward	WI	Aug. 28, 1941
OR 4-8	90	15.4	9.0	70,000 (8.2)	Golconda	IL	Oct. 03, 1910
SW 2-1	114	13.9	13.9	30,000 (4.2)	nr Neosho Falls	KS	Sept. 11, 1926
MR 1-3A	30	12.1	12.1	7,200 (4.2)	Blanchard	IA	July 06, 1898
MR 2-22	102	12.5	11.9	19,900 (3.8)	Warrensburg	MO	Aug. 25, 1919
MR 4-3	78	12.3	12.3	84,000 (3.2)	Greeley	NE	June 04, 1896
MR 6-2	96	12.2	11.2	16,000 (4.1)	Lindsborg	KS	Oct. 18, 1941
UMV 3-29	15	12.0	12.0	20,000 (2.6)	nr Dumont	IA	June 25, 1951
GL 2-29	120	12.4	12.4	58,000 (3.9)	nr Merrill	WI	July 19, 1912
MR 1-1	96	12.2	7.6	110,000 (5.6)	Phillipsburg	MO	Dec. 16, 1895
MR 1-23	96	11.1	10.8	40,000 (3.8)	Nemaha	NE	July 13, 1907
MR 2-9	114	11.4	7.1	48,000 (4.3)	Maryville	MO	July 11, 1915
MR 2-11	96	11.2	11.2	24,000 (4.0)	Moran	KS	Sept. 06, 1915
MR 3-7	168	11.8	7.8	97,000 (4.6)	Lacona	IA	June 10, 1926
MR 3-20	60	11.2	9.9	60,000 (5.1)	Lebo	KS	Nov. 15, 1928
UMV 2-5	12	12.0	12.0	20,000 (3.9)	nr Bonaparte	IA	June 09, 1905
UMV 2-8	66	11.2	8.8	27,000 (5.7)	Bethany	MO	July 04, 1909
UMV 3-20B	186	11.3	8.4	80,000 (5.6)	Galesburg	IL	Sept. 30, 1941
UMV 3-21	42	11.7	11.0	12,600 (3.4)	Thompson Farm	MO	July 07, 1942
GL 2-12	120	11.2	8.9	67,000 (4.2)	Medford	WI	June 03, 1905
MR 2-7	120	10.6	6.8	45,000 (5.1)	Lexington	MO	May 25, 1915
MR 3-8	144	11.0	7.2	177,000 (4.4)	Clarinda	IA	Aug. 31, 1926
MR 3-28B	168	10.9	7.6	50,000 (5.7)	Chanute	KS	May 27, 1935
LMV 1-13A	60	10.6	7.6	84,000 (5.1)	Steelville	MO	Oct. 25, 1919
UMV 2-14	63	10.5	9.6	70,000 (3.3)	Washington	IA	June 12, 1930
GL 3-11	42	11.0	11.0	20,000 (3.8)	Libertyville	IL	June 29, 1938
MR 1-21A	102	10.2	8.6	24,300 (3.6)	Warsaw	MO	Aug. 22, 1906
MR 3-6	48	10.1	8.9	45,000 (3.7)	Lockwood	MO	Sept. 20, 1925
UMV 1-8	108	10.1	7.6	50,000 (3.1)	Newfolden	MN	July 01, 1901
UMV 2-30	24	11.0	11.0	10,400 (2.8)	Oxford Junction	IA	June 25, 1944
LMV 1-3A	84	10.3	8.4	20,000 (5.7)	Sikeston	MO	Sept. 28, 1898
GL 4-5	66	10.2	10.0	15,000 (4.8)	Butternut	WI	July 25, 1897
MR 2-13	126	9.4	6.8	150,000 (5.4)	Ironton	MO	Jan. 26, 1916
MR 3-19	102	9.8	6.0	47,000 (4.9)	Centerville	IA	Sept. 10, 1928
MR 6-3	24	10.9	10.9	5,000 (3.6)	Ballard	MO	June 03, 1943
UMV 1-3	102	9.6	7.1	30,000 (3.6)	Pine River Dam	MN	June 02, 1898
SW 1-25	138	9.4	7.1	70,300 (4.5)	Wichita	KS	June 05, 1923
MR 1-16A	120	9.6	8.2	45,000 (4.1)	Eldorado	KS	June 28, 1905
UMV 1-15	114	9.3	7.4	40,000 (3.8)	Dodgeville	WI	Sept. 11, 1915
UMV 1-25	108	9.7	6.3	40,000 (4.3)	Woodville	WI	Sept. 15, 1942
GL 2-22	90	9.3	7.9	50,000 (3.9)	West Bend	WI	Aug. 03, 1924
MR 6-1	72	9.3	8.9	35,000 (3.5)	Clifton Hill	MO	June 23, 1942
UMV 1-20	120	9.0	6.2	70,000 (3.7)	Baudette	MN	July 11, 1937
UMV 2-3	96	9.0	6.4	48,600 (4.4)	Reeds Landing	MN	Sept. 11, 1903
UMV 2-15	24	9.0	9.0	13,000 (4.4)	Gorin	MO	June 28, 1933
UMV 3-28	30	10.1	10.1	10,500 (4.2)	nr Mifflin	WI	July 15, 1950
GL 2-21	84	9.0	7.5	45,000 (3.5)	Wrightstown	WI	June 08, 1922
MR 1-24	144	9.0	5.1	100,000 (4.0)	Frankfort	KS	June 04, 1908
MR 1-28	78	9.0	8.1	39,000 (3.5)	Topeka	KS	Sept. 06, 1909
MR 3-1A	78	9.5	9.0	3,900 (4.5)	Medicine Lodge	KS	Sept. 29, 1923
MR 3-29	30	10.0	10.0	14,000 (3.4)	nr Sharon Spr.	KS	May 30, 1938
UMV 2-1	78	9.1	6.3	118,000 (4.6)	Warrenton	MO	Dec. 31, 1896
UMV 2-22	30	9.0	9.0	23,400 (2.9)	Gander	IA	July 25, 1940
UMV 4-11	54	9.2	9.2	28,500 (3.7)	Galva	IL	Aug. 18, 1924
MR 7-9	30	9.3	9.3	8,300 (4.2)	Jerome	IA	July 16, 1946
GL 2-30	54	9.1	8.9	5,000 (4.2)	Viroqua	WI	July 21, 1917
MR 3-11	54	9.0	8.9	13,300 (3.3)	Channte	KS	April 07, 1927
MR 2-23	66	9.1	8.7	58,350 (4.2)	Bruning	NE	Sept. 16, 1919
MR 1-29	138	9.0	6.1	92,000 (4.8)	Neosho	MO	Nov. 10, 1909
MR 6-13	42	9.3	5.8	3,000 (3.4)	near Pierce	NE	May 10, 1944
MR 6-16	36	9.3	9.1	5,100 (2.3)	near Bagnell	MO	Aug. 01, 1944
MR 7-16	10	9.4	9.4	220 (4.3)	near Gering	NE	June 17, 1947

Numbers in parenthesis are associated average depths in inches. For metric conversion, use 1 inch = 25.4 mm and 1 mi^2 = 2.59 km^2.

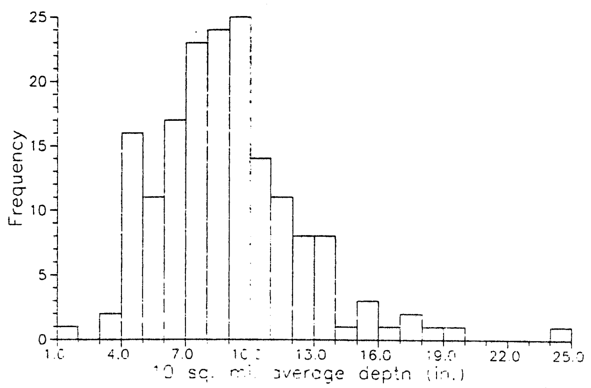

Fig. 1. Empirical distribution of total storm center depth of all midwestern storms found in the catalog for the period 1891– 1951.

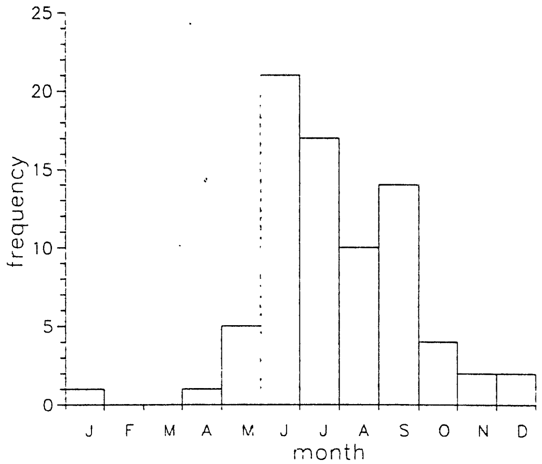

Fig. 2. Seasonal distribution of all 77 storms.

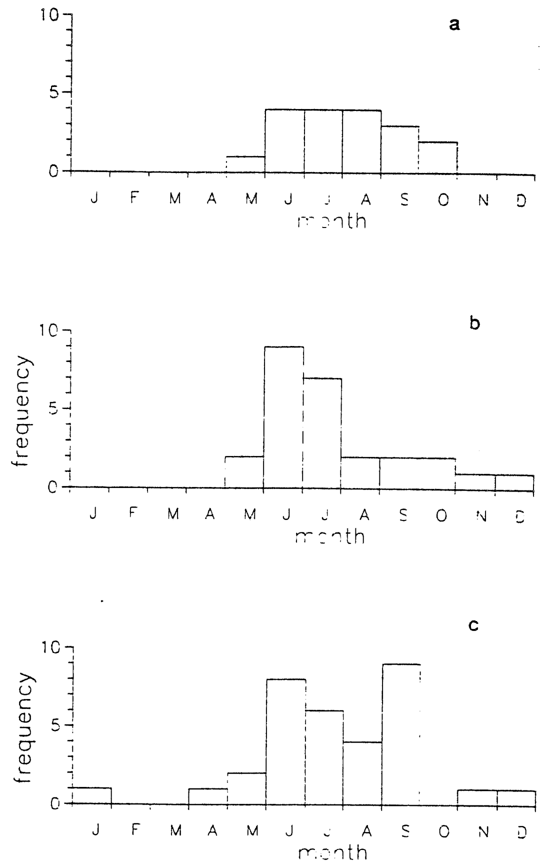

Fig. 3. Seasonal distribution of extreme storms in sets 1, 2, and 3, respectively. (See text for definition of these sets.)

summer months, with almost 80% of them occurring during the months of June–September. This finding is consistent with observations of other investigators [see *Wallace and Hobbs*, 1977, Figure 1.21; *Huff and Semonin*, 1960]. From the seasonal distribution of the storms in sets 1–3 (Figures 3*a*–3*c*), it is observed that the winter storms tend to be less severe, at least in terms of maximum recorded depths. The seasonal distribution of the storms in sets 4–6 (Figures 4*a*–4*c*) indicates that storms of medium duration tend to occur more frequently in the late summer months, while storms of lower duration tend to occur more frequently in the early summer months.

The chronological distribution of the extreme midwestern storms is shown in Figure 5. At the very beginning of the record, there is a 3-year stretch (1892–1894) without a single occurrence of an extreme storm. This may be due to record incompleteness, since such a gap is not observed even during the 1930s, one of the driest periods in the history of the Midwest. Thus it was assumed that the record is complete for the period 1895–1951. For that period, no apparent clustering or nonstationarity in the annual occurrence of storms is observed. In view of the seasonality of the storm occurrences, the storm occurrence process $N(t)$ on the interval of 1 year $(0,1]$ is hypothesized to be a nonstationary Poisson process with intensity function $\lambda(t)$. It follows that the annual occurrence rate Λ is given by

$$\Lambda = \int_0^1 \lambda(u)du \tag{1}$$

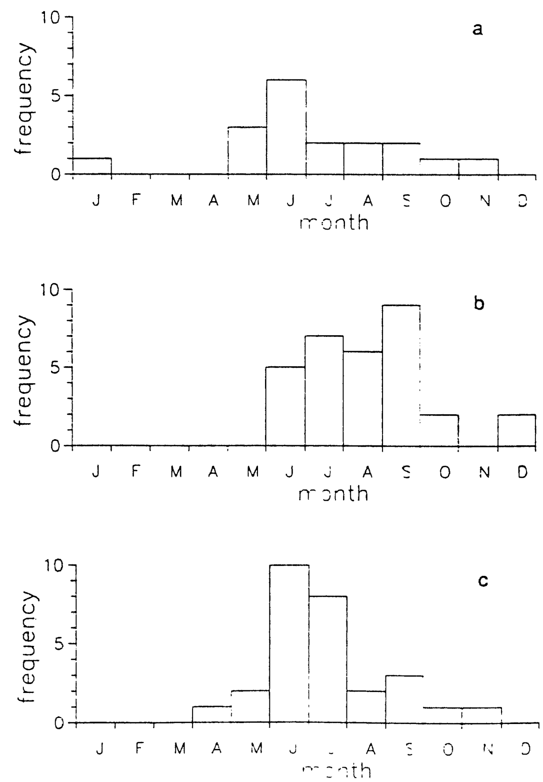

Fig. 4. Seasonal distribution of extreme storms in sets 4, 5, and 6, respectively. (See text for definition of these sets.)

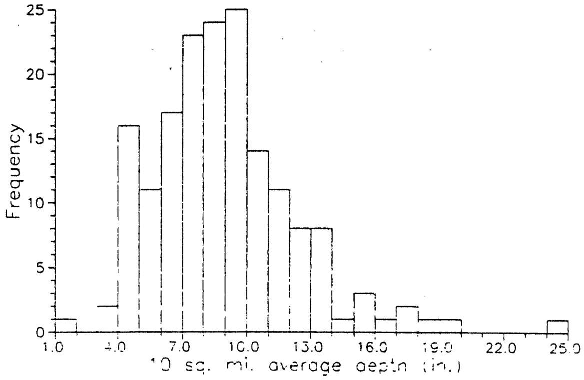

Fig. 1. Empirical distribution of total storm center depth of all midwestern storms found in the catalog for the period 1891– 1951.

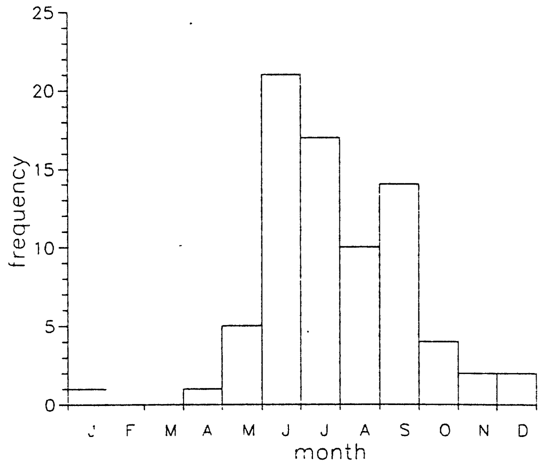

Fig. 2. Seasonal distribution of all 77 storms.

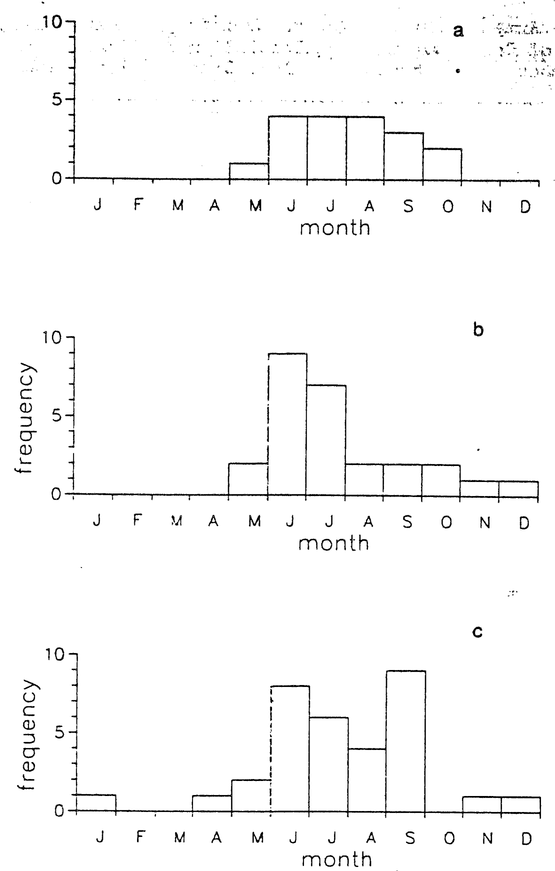

Fig. 3. Seasonal distribution of extreme storms in sets 1, 2, and 3, respectively. (See text for definition of these sets.)

summer months, with almost 80% of them occurring during the months of June–September. This finding is consistent with observations of other investigators [see *Wallace and Hobbs*, 1977, Figure 1.21; *Huff and Semonin*, 1960]. From the seasonal distribution of the storms in sets 1–3 (Figures 3*a*–3*c*), it is observed that the winter storms tend to be less severe, at least in terms of maximum recorded depths. The seasonal distribution of the storms in sets 4–6 (Figures 4*a*–4*c*) indicates that storms of medium duration tend to occur more frequently in the late summer months, while storms of lower duration tend to occur more frequently in the early summer months.

The chronological distribution of the extreme midwestern storms is shown in Figure 5. At the very beginning of the record, there is a 3-year stretch (1892–1894) without a single occurrence of an extreme storm. This may be due to record incompleteness, since such a gap is not observed even during the 1930s, one of the driest periods in the history of the Midwest. Thus it was assumed that the record is complete for the period 1895–1951. For that period, no apparent clustering or nonstationarity in the annual occurrence of storms is observed. In view of the seasonality of the storm occurrences, the storm occurrence process $N(t)$ on the interval of 1 year (0,1] is hypothesized to be a nonstationary Poisson process with intensity function $\lambda(t)$. It follows that the annual occurrence rate Λ is given by

$$\Lambda = \int_0^1 \lambda(u)du \tag{1}$$

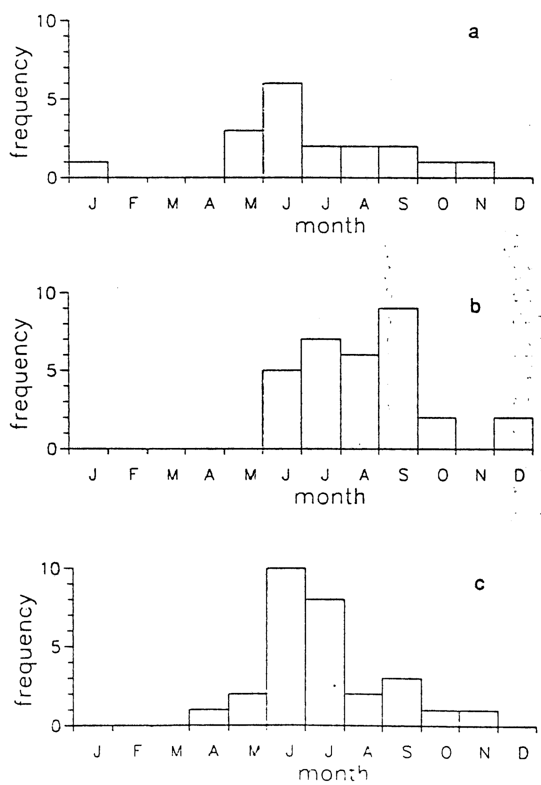

Fig. 4. Seasonal distribution of extreme storms in sets 4, 5, and 6, respectively. (See text for definition of these sets.)

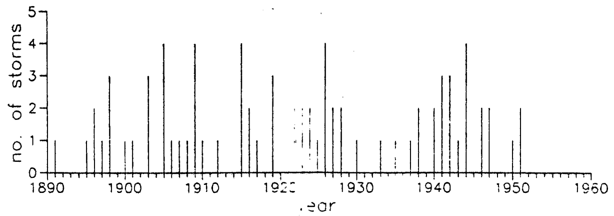

Fig. 5. Chronological distribution of the 77 analyzed extreme midwestern storms.

and the number of storm occurrences during a year, $N(1)$, follows a Poisson distribution with parameter Λ, i.e.,

$$p(N(1) = k) = \Lambda^k e^{-\Lambda}/k! \tag{2}$$

The mean annual occurrence rate Λ was estimated for this process to be 1.33 storms/year and the Poisson hypothesis was accepted at the 90% significance level (see, for example, *Cox and Lewis* [1978] for statistical tests on the Poisson hypothesis).

The frequency distribution of the starting time of the storms is shown in Figure 6. The starting times are taken from the storm catalog, where they are reported either in hourly increments or at 6-hour intervals (i.e. 12 midnight, 6 A.M., 12 noon, 6 P.M.) depending on the reading times of the rain gages. This discretized form of the data gives rise to peaks at certain times, as observed in Figure 6. It appears that most of the extreme midwestern storms occur in the late evening or early morning hours with a maximum number of occurrences at midnight. This finding is consistent with observations of other investigators (see, for example, *Wallace and Hobbs* [1977, Figure 1.23], *Huff and Semonin* [1960], *Maddox* [1980], *Maddox et al.* [1979], among others). *Huff and Semonin* [1960] presented a study of the hydrometeorological synoptic conditions of severe storms in Illinois and provided a physical explanation of the pronounced diurnal variability and frequent night occurrence of the unusually severe rainstorms in the Midwest. In brief, severe midwestern storms are usually produced by convective systems which start in the afternoon with the assistance of diurnal heating and develop into widespread and intense systems by late afternoon or early evening. When such well developed systems, laden with moisture, move into a zone of instability, unusually heavy rainstorms are likely.

Maddox [1980] found that mesoscale convective complexes (MCCs) are likely to play a large role in the nocturnal maxima of thunderstorms and precipitation events over the central United States. In particular, he observed that although the first storms typically developed during the afternoon, the transition to large, highly organized mesosystems did not usually occur until early evening. Most of the systems reached their maximum size (as indicated by satellite imagery) after midnight and continued into the morning hours. Also, *Maddox et al.* [1979] found that significant flash floods in the eastern two- thirds of the United States usually occurred during nighttime hours.

SPATIAL DISTRIBUTION OF THE STORM CENTERS

For studies involving storm regionalization, such as the storm transposition approach [e.g., *Foufoula-Georgiou*, 1989a], there is a need to obtain the probability of a storm occurring in a region different from the one where it actually occurred. Most studies assume a climatologically or statistically homogeneous region within which storms can be transposed with the same probability (i.e., constant spatial rate of storm occurrences). Alternatively, one could work with a larger statistically inhomogeneous region within which extreme storms can occur with different probabilities (i.e., spatially variable rate of occurrence). The latter approach would provide a larger data set for use in regionalization or storm transposition studies; it would require, however, the characterization of the spatial distribution of the positions of extreme storms.

The spatial distribution of the storm centers of all 77 extreme midwestern storms is shown in Figure 7. A preferred centering of extreme storms in the central, south, and northeast part of the nine-state region is apparent. For this data set, no extreme storm is centered in the states of North and South Dakota, and the states of Minnesota and Illinois have only four extreme storm centers each. This preferred storm location pattern becomes more pronounced for the most extreme storms, as can be seen from Figures 8*a*–8*c* for storm sets 1–3, and Figures 9*a*–9*c* for storm sets 4–6. The empirically observed strong spatial inhomogeneity, may be due in part to small or incomplete samples. However, several studies [e.g., *Fritsch et al.*, 1986] provide evidence that normal summer precipitation and precipitation from mesoscale weather systems is significantly lower as one moves to the north part of the studied midwestern area, a finding that supports the observed spatial inhomogeneity. Partial meteorological explanations for this inhomogeneity may be sought

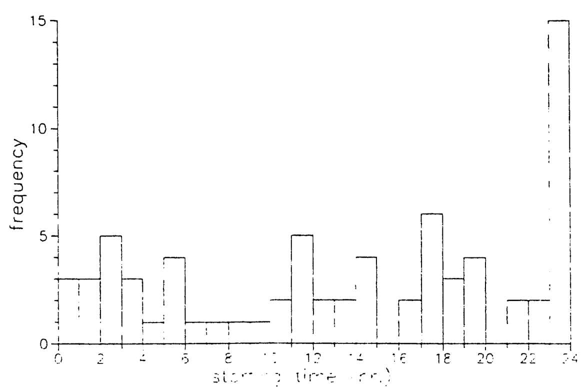

Fig. 6. Empirical distribution of the starting time of all 77 storms.

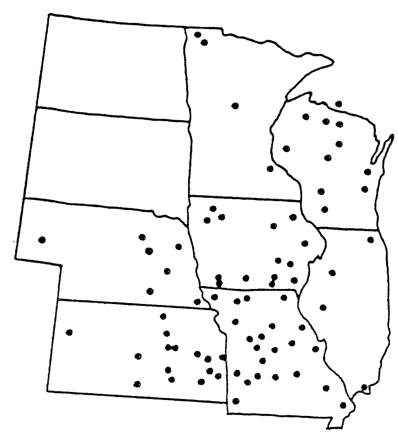

Fig. 7. Spatial distribution of the storm centers of all 77 storms over the midwest region.

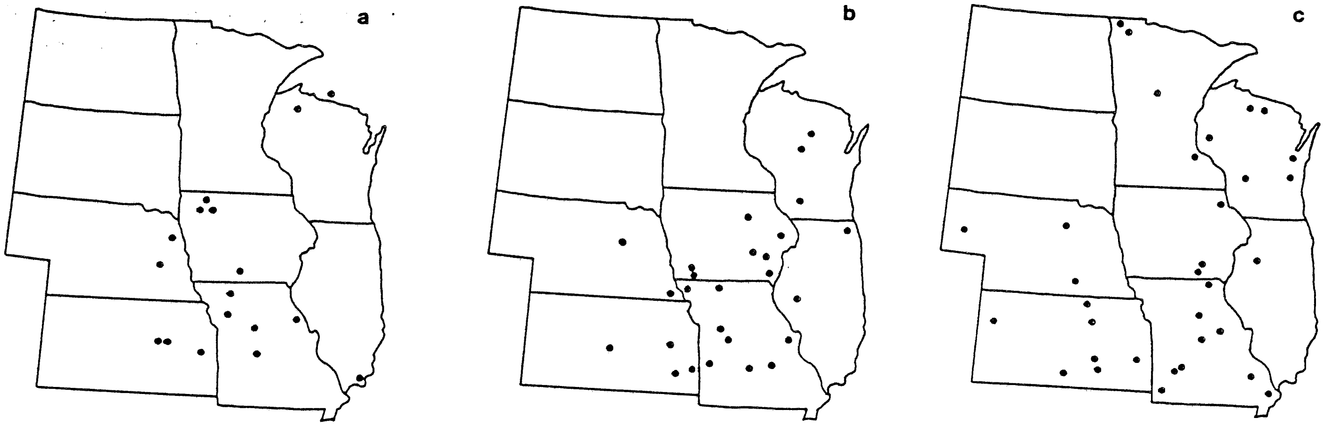

Fig. 8. Spatial distribution of the storm centers of set 1, 2, and 3, respectively. (See text for definition of these sets.)

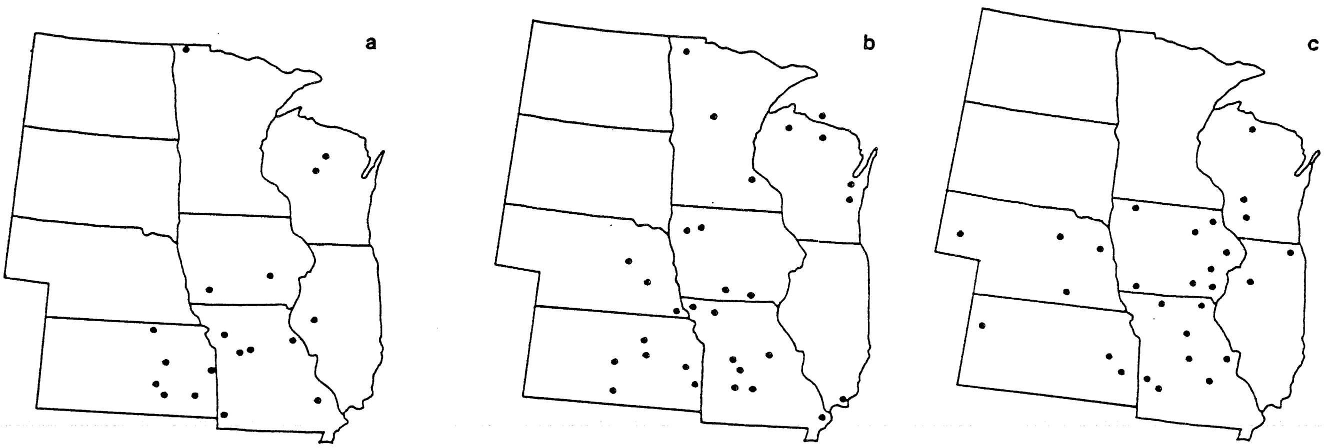

Fig. 9. Spatial distribution of the storm centers of set 4, 5, and 6, respectively. (See text for definition of these sets.)

by connecting it to the observed movement characteristics of mesoscale convective complexes [e.g., *Maddox et al.*, 1982].

A useful description of the spatial occurrence of storms is in terms of their latitudinal and longitudinal frequency distributions, as shown in Figure 10. This type of representation, commonly used in earthquake occurrence studies [e.g., *Veneziano and Van Dyck*, 1987], may be useful in defining the limits of statistically homogeneous areas, or in estimating the spatially variable rate of occurrence, $\lambda(x, y)$, of an inhomogeneous spatial Poisson process on the basis of the two-dimensional (latitudinal and longitudinal) frequency distribution of the storm occurrences (as shown in Figure 10).

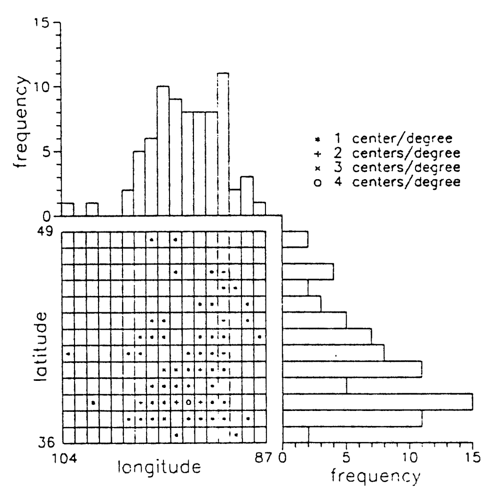

Fig. 10. Spatial occurrence of storm centers as a function of latitude and longitude.

Storm Shape

The total storm isohyetal patterns usually tend to be very complex. *Huff* [1967] observed that for storms over Illinois, elliptical isohyetal patterns predominate, and there is a trend for the patterns to become more complex with increased storm duration and rainfall volume. In this analysis we have assumed that an elliptical shape can reasonably approximate all storms. The parameters of the ellipse have been estimated using the total storm isohyetal patterns published by the U.S. Army Corps of Engineers and usually reported up to the contour of 3 inches (7.6 cm). The fitting consisted of graphically centering an ellipse over the storm isohyetal pattern until a satisfactory c value, where c is the ratio of the major axis to the minor axis of the ellipse, was obtained. The c values were estimated to the nearest 0.5 increment. This method is admittedly subjective and approximate. However, in hydrologic studies involving storm shape, the accuracy of the results may not be as critical as it first appears. As it was shown by *Foufoula-Georgiou* [1989a], misspecification of the storm shape (e.g., specifying $c = 2.5$ instead of $c = 3.0$) does not seem to result in significant differences, as far as the mean and variance of the catchment wetted area and average catchment depth are concerned. However, it was shown that the differences are significant if the storm shape is specified as circular (a common approximation of several previous studies) when it is actually elliptical with a major to minor axis ratio greater than or equal to 2.

Figure 11 shows the empirical frequency distribution of c for all 77 storms, and Table 2 gives the mean and standard deviation of c for sets 1–6. It appears that at larger depths the storms tend to be more elongated (i.e., larger

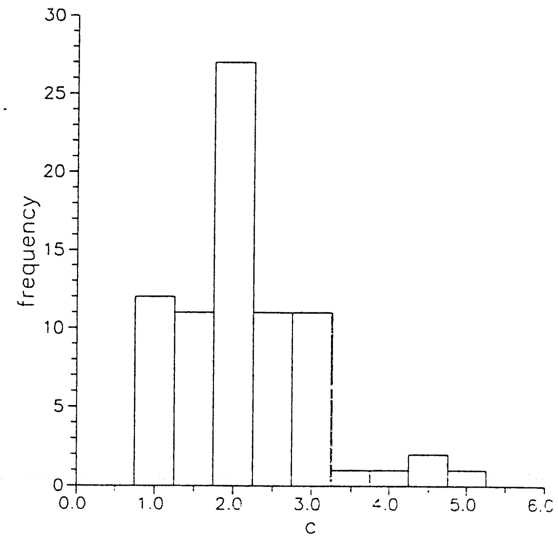

Fig. 11. Empirical distribution of the storm shape parameter c (ratio of major to minor axis).

TABLE 2. Statistics of the Storm Shape Parameter c for Storm Sets 1–6 and for all 77 Storms

Storm Set	$E(c)$	$s(c)$
1	2.44	0.566
2	2.12	0.725
3	2.03	1.038
4	1.97	0.696
5	2.19	0.760
6	2.23	1.032
All 77	2.16	0.852

c values). Also, less extreme storms tend to have highly variable shapes, e.g., some of them are nearly circular, and some are very elongated elliptical. For storms of longer duration the variability of the shape parameter is small, while the storms of shorter duration tend to be more variable in shape. Also, as the duration increases, an increase in the number of circular storms is apparent, although the mean c value is still close to a 2:1 ratio. This analysis points out the importance of considering the storm shape to be elongated, and not circular, in studies involving storm regionalization and basin runoff production.

STORM ORIENTATION AND STORM MOVEMENT DIRECTION

With the storm being more elliptical than circular in shape, the orientation of the storm with respect to the basin becomes very critical as well. For example, if the storm's major axis is aligned with the main channel of the basin, one would see a significantly higher flood peak than if the major axis were perpendicular to this channel. Also, basins generally are not circular in shape. In fact, empirical evidence suggests that as the area of a catchment increases, there is a tendency toward an elongation of the shape of the catchment. This geometrical dissimilarity of basin shapes is described by the empirical relationship $L = cA^{0.568}$ where L is the main channel length and A is the catchment area [e.g., *Eagleson*, 1970, p. 378]. Therefore, since catchments are generally not circular, the storm shape and orientation relative to those of the catchment will have a significant effect on the percent coverage of the basin and thus on the produced runoff.

Unfortunately, the storm catalog data do not provide enough information for a study of storm orientation. Previous investigators, however, have provided evidence of a preferred storm orientation of extreme midwestern storms. *Huff and Semonin* [1960] studied 262 Illinois storms for the years 1914–1957 with a 2-day duration and an average 10,000 mi^2 (25,900 km^2) rainfall depth exceeding 1 inch (2.5 cm). The frequency histogram of the orientation of all these storms is shown in Figure 12b and for storms with an average 10 mi^2 depth greater than 9.9 inches (25 cm) is shown in Figure

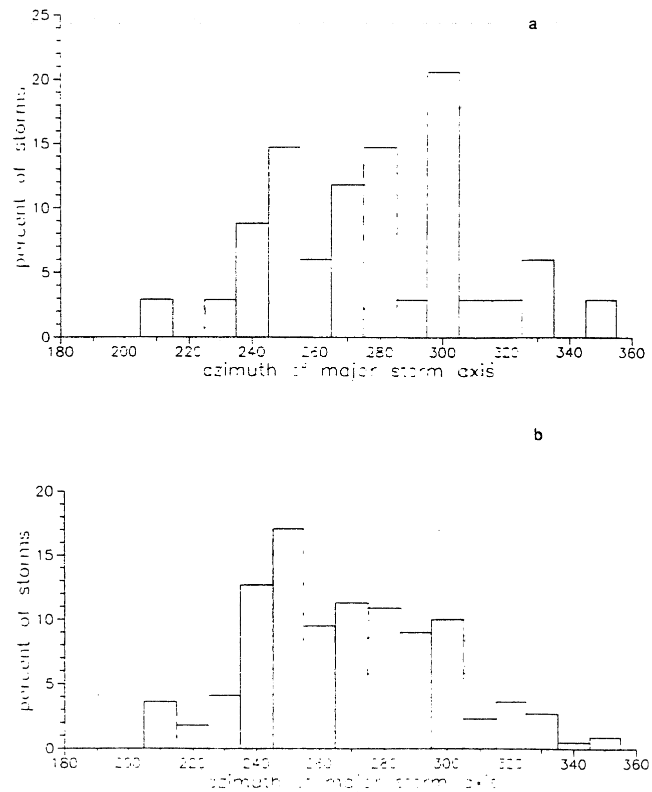

Fig. 12. Empirical distribution of storm orientations for extreme Illinois storms over the period 1914–1957. (*a*) Two-day storms with an average 10 mi^2 depth greater than 9.9 inches. (*b*) Two-day storms with an average 10,000 mi^2 depth exceeding 1 inch. (Reproduced from results of *Huff and Semonin* [1960].)

12a (79.5% of these storms were found to have an orientation between 235° and 305°). (An orientation of 200° indicates that the storm's major axis is oriented on a line from 200° to 20°, where the angles are measured clockwise from the north.) Another study by *Huff* [1967] of 261 less extreme storms from 1955 to 1966 in east central Illinois indicated that 68% of the storms had an orientation from SSW to WSW. Also, as the intensity and areal extent of a flood-producing storm increased, the movement of the storm, and consequently its core orientation, veered from SW-WSW toward the west.

Gupta [1972] used *Huff*'s [1967] orientation data in a storm transposition study for estimating extreme floods and their probabilities. He fit a Beta distribution

$$f(\theta) = \frac{1}{B(a,b)}\theta^{a-1}(1-\theta)^{b-1} \quad (3)$$

to the standardized storm orientation $\theta = \phi/\pi$, where ϕ is the actual storm orientation in radians, a and b are the distribution parameters, and $B(\ )$ is the beta function.

With respect to the storm movement direction, *Huff* [1978] observed that for extreme Illinois storms, the storm orientation and direction were closely related to the wind aloft and to the orientation and movement of the squall lines which were almost always present in the large mesoscale storms. For example, the medians for the squall line orientation and layer winds (850–500 mbar) were identical (255° with a 90% range of 230°–280°), and the median orientation of the surface rainfall pattern departed 10° from the squall line orientation and in nearly all storms was to the right (veering) of the squall lines (265° with a 90% range of 240°–290°). Also, the squall lines had the tendency to rotate anticyclonically and to slow down in speed from a median of 20 knots (10 m/s) outside the rain zone to 8 knots (4 m/s) within the rain zone. It should be noted that several of the above synoptic hydrometeorological characteristics have been observed in mesoscale convective complexes (MCCs) over the central Plains of the United States [see, *Maddox*, 1980; *Maddox et al.*, 1982; *Rodgers et al.*, 1983, 1985; *Augustine and Howard*, 1988].

STORM AREAL EXTENT

Due to the spatial resolution of the rain gage network, it is usually difficult to accurately specify the total areal extent of a storm. If one defines the total storm areal extent as the area enclosed within the contour of 1 inch, then this area is usually very irregular and is not reported in the storm catalog. In order to make a more meaningful comparison of areal extent of extreme storms, we have used here a representative storm area, called the "characteristic storm area," A_{ch}, which is defined as the area over which the total average depth is approximately equal to one-half of the total depth at the storm center, i.e.,

$$\bar{d}(A_{ch}) = d_o/2 \quad (4)$$

[see *Boyer*, 1957]. A_{ch} can be estimated from the DAD tables given in the storm catalog by interpolating between the two areal values associated with the depths just above and below the depth value of $d_o/2$. As before, the value of $\bar{d}(10)$ was used instead of the value of d_o. Seven storms from the set of 77 had to be omitted from the analysis because the value of $\bar{d}(10)/2$ fell outside the range of the depths reported in the DAD tables.

The empirical distribution of the logarithms of A_{ch} is given in Figure 13. A two-parameter lognormal distribution given by

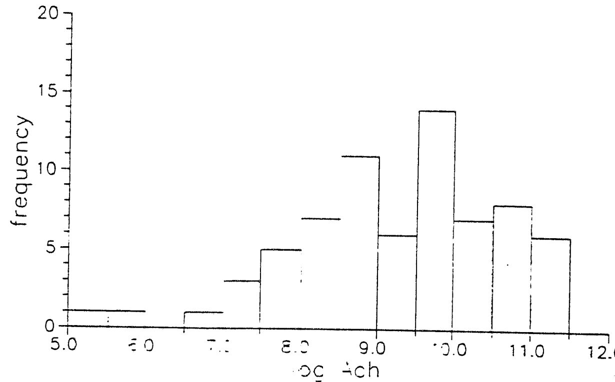

Fig. 13. Empirical distribution of the logarithms of the characteristic area A_{ch} for all 77 storms.

$$f(A_{ch}) = \frac{1}{A_{ch}\sigma_y\sqrt{2\pi}} e^{-\frac{[\ln A_{ch} - \mu_y]^2}{2\sigma_y^2}} \quad (5)$$

where μ_y and σ_y are the mean and standard deviation, respectively, of the logarithms of A_{ch} ($y = \ln A_{ch}$), was fitted to this frequency histogram. It was found that with $\hat{\mu}_y = 9.257$ and $\hat{\sigma}_y = 1.326$. the two-parameter lognormal distribution was accepted at the 95% confidence level. The estimates of the mean and standard deviation of A_{ch} were 20,295 and 21,710 mi^2 (52,564 and 56,229 km^2), respectively, illustrating the wide variations possible in the areal extent of extreme storms.

It is interesting to note that a limiting relationship appears to exist between storm areal extent and storm shape. For example, a scattergram of the characteristic storm area and the storm shape parameter (Figure 14) suggests, within the accuracy limits of the parameters, an envelope curve having a linear relationship between c and $\ln A_{ch}$. Such limiting relationships are interesting and often helpful in extreme storm analysis.

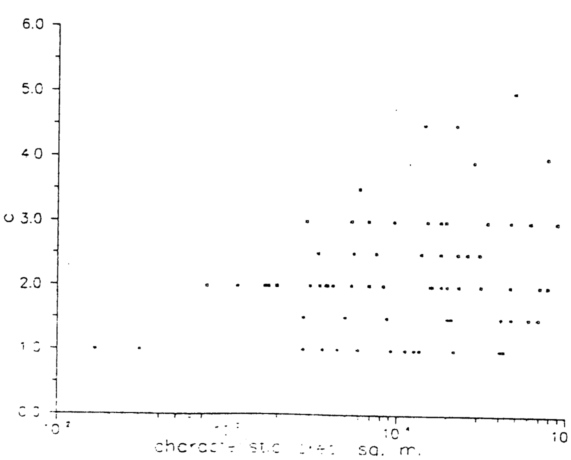

Fig. 14. Storm shape parameter versus storm characteristic area for all 77 midwestern storms.

STORM DURATION

A common measure of storm duration is the total storm duration, t_r, defined as the time between the beginning of the storm and the end (dissipation) of the storm. The t_r can be estimated as the time between which the increase in depth is greater than 0.01 inches (0.025 cm) at at least one point within the storm. The frequency histogram of the total storm duration, t_r, as reported in the storm catalog for all the 77 analyzed storms, is shown in Figure 15*a*. The mean storm duration was 85.48 hours, and the standard deviation 41.92 hours. A two-parameter Gamma distribution, given by

$$f(t_r) = \frac{1}{\theta^k \Gamma(k)} t_r^{k-1} e^{-t_r/\theta} \tag{6}$$

was fit to this frequency distribution and the method-of-moments parameter estimates were $\hat{\theta} = 20.56$ and $\hat{k} = 4.16$. Using the chi-square and Kolmogorov-Smirnov tests, this distribution was accepted at the 95% confidence level.

The duration of rainfall varies not only from storm to storm but also within the storm. As *Milly and Eagleson* [1988] comment, the variability of the total storm depth within the storm is not only due to the variability of rainfall intensity but also to the variability of rainfall duration. That is, lower depths at large distances from the center are due to a combination of lower rainfall intensities and shorter rainfall durations. To get an idea of the variability of the rainfall duration within a storm, we define herein the "storm center duration," t_{ro}, as the time from the beginning of the storm until the total depth at the storm center (i.e., the point of maximum recorded depth) does not change by more than a prespecified small amount (e.g., 0.01 inches) during the duration of the storm

$$t_{ro}: \ \{d_o(t_{ro} + \Delta t) - d_o(t_{ro}) < 0.01\} \tag{7}$$

Assuming stationarity of the storm, the storm center duration was estimated using the 10 mi^2 average depth reported in the DAD tables of the storm catalog. The empirical distribution of $\hat{t}_{ro}$ is shown in Figure 15*b*. The artificial peaks around certain times are due to the fact that the published DAD data are not continuous at the 6-hour level and in many cases, not even at the 12-hour level.

As a crude measure of the variability of rainfall duration within the extreme midwestern storms, we looked at the moments of t_{ro}/t_r. This ratio is usually assumed to be one, but for the analyzed storms it has a mean of 0.730 and a standard deviation of 0.242. From the above analysis, one can get a general idea of just how variable the duration of rainfall can be over the area of a storm, and that in many cases it is important to take this storm feature into account when developing a model. For example, due to this variability, the probability distribution of the rainfall intensity would not be the same as the probability distribution of the storm depths, as is usually assumed in many studies and models.

TOTAL STORM DEPTH AND DEPTH-AREA RELATIONSHIPS

The empirical distribution of the total storm center depth d_o, conditioned on $d_o \geq 9.0$ inches, is shown in Figure 16. A shifted exponential distribution, given by

$$f(d_o) = \frac{1}{\alpha} e^{-\frac{d_o - u}{\alpha}} \tag{8}$$

where u is the cutoff level of 9 inches, was fit to this histogram. The hypothesis of a shifted exponential distribution with $\hat{\alpha} = 2.56$ inches (6.5 cm) was accepted at the 95% confidence level (using the Kolmogorov-Smirnov and chi-square tests).

The description of the spatial distribution of rainfall within a storm is very important in many hydrologic applications. It is well known that the distribution of runoff is affected not only by the total volume of rainfall over the basin, but also by its areal distribution [e.g., *Wilson et al.*, 1979]. The detailed description of the spatial rainfall characteris-

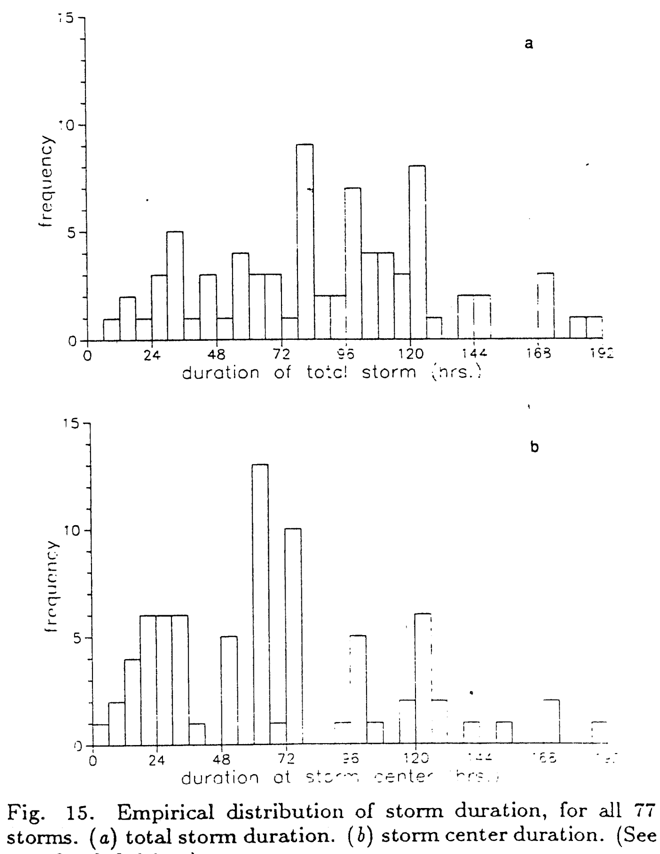

Fig. 15. Empirical distribution of storm duration, for all 77 storms. (*a*) total storm duration. (*b*) storm center duration. (See text for definition.)

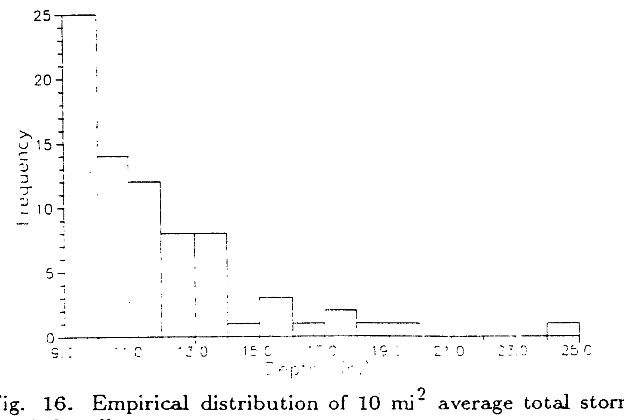

Fig. 16. Empirical distribution of 10 mi^2 average total storm depth for all 77 storms.

tics within a storm would require stochastic representations such as that of *Waymire et al.* [1984]. These models have a physical basis and take into account the empirical evidence [e.g., *Austin and Houze*, 1972; *Hobbs and Locatelli*, 1978] of the preferred hierarchical structure of the smaller higher intensity rainfall areas within a synoptic area. For design purposes, however, it has been customarily assumed, primarily as an extra safety factor, that the variable of interest is the maximum average storm depth over an area equal to the area of the catchment. Thus emphasis has been given here to relationships describing the average storm depth as a function of the smallest area over which this average storm depth can be observed within the storm. In other words, the highly irregular and spotty rainfall field is conceptualized here as a single-center pattern of a given geometrical shape with concentric and geometrically similar isohyets. Under this conceptualization, the spatial rainfall distribution is described by what is known as the depth-area curve which is reported in the storm catalog and is used for design purposes.

For the 77 extreme midwestern storms (which were selected as to have a total 10 mi^2 average depth exceeding 9 inches), the mean, median, maximum, and minimum values of $\bar{d}(A)$, the average rainfall depth over an area A, versus A are plotted in Figure 17 for the maximum 24-hour average storm depth. It is observed that the variability of the maximum 24-hour average depth $\bar{d}(A)$ (conditional on the total 10 mi^2 average depth exceeding 9 inches) decreases with increasing area and the distribution of $\bar{d}(A)$ tends to become more symmetric for areas of 10^3–10^4 mi^2 or larger. For smaller areas the distribution of $\bar{d}(A)$ is highly positively skewed. This is often the result of a few very extreme depths as shown in Figure 18 for the 10 mi^2 maximum 24-hour average depth. In general, it appears that the extreme storms with the very high center depths tend to decrease in depth very rapidly as their areal extent increases.

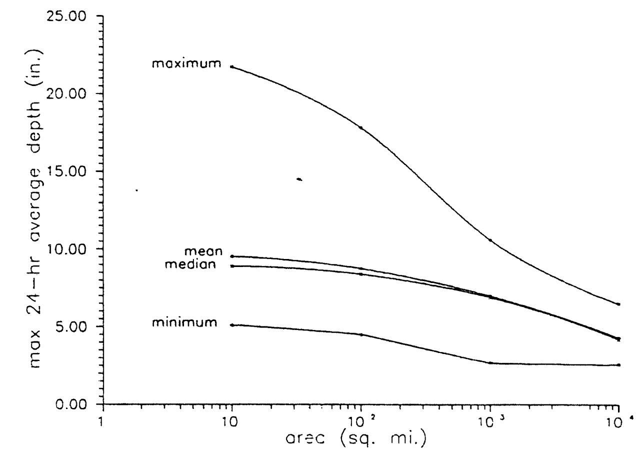

Fig. 17. Mean, median, maximum, and minimum values of the maximum 24-hour average depth over an area A versus area A for all 77 storms.

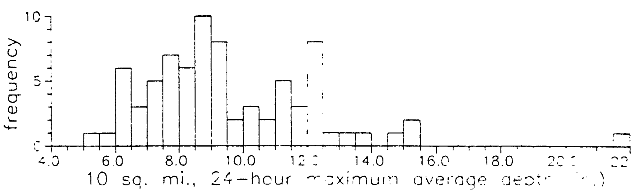

Fig. 18. Empirical distribution of the maximum 24-hour, 10 mi^2 average depth for all 77 storms.

Based on the assumption of single-center storms with concentric geometrically similar isohyets, several models for the depth-area relationship of a storm have appeared in the literature (see, e.g., *Court* [1961] for a review). The most commonly used relationship is one where the average depth decreases exponentially with a fractional power of the area. This relationship was given by *Horton* [1924], as

$$\bar{d}(A) = d_o e^{-kA^n} \tag{9}$$

where d_o is the storm center depth and $\bar{d}(A)$ is the average storm depth over an area A about the storm center. *Horton* [1924] provides a physically based justification of the form of this relationship. A similar relationship, given by *Huff et al.* [1958] and *Huff and Semonin* [1960], is

$$\log \bar{d}(A) = a - bA^n \tag{10}$$

This relationship has the same form as (9), but it is more flexible in the sense that it does not rely on the value of d_o, which is usually unknown. Equation (10) was fit to the maximum 24-hour depth-area data for all 77 extreme storms. Areas of 10–10,000 mi^2 were used in the fitting; however, for larger storms, where the 3-inch isohyet enclosed an area substantially larger than 10,000 mi^2, areas larger than 10,000 mi^2 were also included in the fit. The duration of 24 hours was selected, since that is considered to be a typical time of concentration for many basins of hydrologic interest. Similar analyses can be performed for the depth-area relationships at other durations. A nonlinear weighted least squares method, with weights inversely proportional to the area, was used. In that way, a better fit was obtained at larger depths/smaller areas, since underestimation of these values can have important impacts on hydrologic design in small basins.

The marginal empirical distributions of the estimates of the parameters a, the logarithm of b, and n are shown in Figures 19*a*–19*c*. Their first three moments and first cross correlation coefficient are given in Table 3 for the whole set of 77 storms and for sets 1–6. As can be seen from Table 3, the commonly assumed relationship of $\bar{d}(A)$ being proportional to the square root of the area A [e.g., *Court* 1961], although justified in terms of average values, fails to account for the considerable variability in the parameter n. Also, the parameters a, b, and n are significantly correlated. In physical terms, these correlations imply that storms with higher center depths (large a) have a rapidly decaying isohyetal profile (larger b and smaller n). This crosscorrelation of the parameters should not be ignored in simulation studies where synthetic storms are generated based on their statistical characteristics.

Court [1961] and *Horton* [1924] have reported average values of $k = 0.0023$ (and $n = 0.56$) for small intense storms over Boston and $k = 0.01$ (and $n = 0.45$) for extreme storms over the eastern half of the United States taken from the Miami Conservancy District records. It is interesting to observe the differences and similarities between these mean values of k and the ones obtained from the set of 77 midwestern storms studied herein. Note that from a comparison of (9) and (10), the parameter k is equivalent to $2.3026b$.

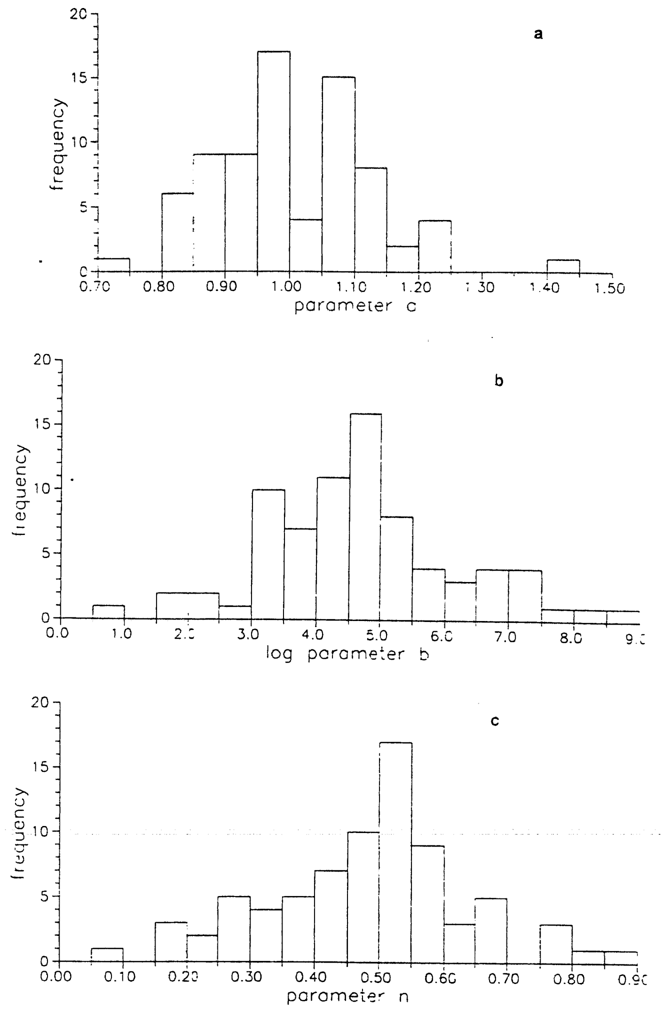

Fig. 19. Empirical distribution of the parameters a, $logb$, and n of the average depth-area relationship $log\bar{d}(A) = a - bA^n$ fit to the maximum 24-hour average depths of all 77 storms.

CONCLUSIONS

Extreme rainstorms play an important role in the design and operation of water resource systems. Due to the lack of complete knowledge of the complex meteorological mechanisms that produce and sustain extreme storms, statistical and correlation analyses are a valuable and complementary tool in identifying regularities of extreme rainfall characteristics. In this paper, we have studied several characteristics of extreme storms centered over a nine-state region in the midwest. The data base used is the extreme storm catalog [*U.S. Army Corps of Engineers*, 1945–]. For the period 1891–1951, 77 storms were identified with their centers within the region of interest and with total storm center depths exceeding 9 inches. First, the occurrence process of extreme storms in space and time was studied. It was found that extreme midwestern storms occur mostly during the summer months and that the number of extreme storms in a year follows a Poisson distribution with a constant parameter $\Lambda = 1.33$ storms/yr. The geographical distribution of the storm centers indicates a spatial inhomogeneity; most extreme storms seem to be centered in the central, south, and northeast part of the studied area. This inhomogeneity is even more pronounced for the very extreme storms. For the nine-state midwestern region, an inhomogeneous spatial Poisson process seems to describe the spatial occurrence of extreme storms. The spatially variable rate of occurrence may be estimated from the longitudinal and latitudinal empirical distribution of the storm center occurrences.

The other extreme storm characteristics studied are storm shape and orientation, total storm center depth, total storm duration, duration at the storm center, storm areal extent, and depth-area relationships. Empirical frequency histograms for these characteristics were obtained, and probability distributions were fit to some of these variables. These probability distributions can provide a basis of empirical modeling and simulation of extreme storms for hydrologic applications. Also, the identified similarities of extreme storm characteristics may promote or complement meteorological studies (such as those by *Heideman and Fritsch* [1984] and *Kane et al.* [1987], among others) that aim at

TABLE 3. Statistics of the Parameter Estimates a, b, and n in the Average Depth-Area Relationship $log\bar{d}(A) = a - bA^n$ fit to the Maximum 24-Hour Average Depths for all 77 Storms and for Sets 1–6

	All 77	Set 1	Set 2	Set 3	Set 4	Set 5	Set 6
$E(a)$	0.994	1.090	1.014	0.930	0.904	1.005	1.038
$s(a)$	0.123	0.144	0.086	0.098	0.096	0.126	0.106
$c_s(a)$	0.531	0.160	-0.333	0.608	0.439	0.179	1.718
$E(b)$	0.017	0.014	0.013	0.021	0.015	0.018	0.019
$s(b)$	0.038	0.021	0.019	0.054	0.026	0.048	0.032
$c_s(b)$	4.611	2.429	2.522	3.631	2.276	4.926	3.019
$E(n)$	0.478	0.477	0.456	0.496	0.444	0.518	0.455
$s(n)$	0.158	0.182	0.133	0.165	0.169	0.167	0.135
$c_s(n)$	-0.090	0.787	-0.506	-0.607	0.695	0.754	0.095
$r_{a,b}$	0.281	0.313	0.114	0.566	0.465	0.207	0.403
$r_{a,n}$	-0.255	-0.360	0.005	-0.327	-0.294	-0.253	-0.443
$r_{b,n}$	-0.647	-0.715	-0.816	-0.718	-0.723	-0.660	-0.683

explaining the characteristics, formation, and development of extreme midwestern storms.

Acknowledgments. This material is based upon work supported by the National Science Foundation under grants CES-8708825 and BSC-8957469.

REFERENCES

Alexander, G. N., Using the probability of storm transposition for estimating the frequency of rare floods, *J. Hydrol., 1*(1),46–57, 1963.

Augustine, J. A., and K. W. Howard, Mesoscale convective complexes over the United States during 1985, *Mon. Weather Rev., 116*(3), 685–701, 1988.

Austin, P. M., and R. A. Houze, Analysis of the structure of precipitation patterns in New England, *J. Appl. Meteorol., 11*(6), 926–935, 1972.

Boyer, M. C., A correlation of the characteristics of great storms, *EOS, Trans. AGU, 38*(2), 233–238, 1957.

Court, A., Area-depth rainfall formulas, *J. Geophys. Res., 66*(6), 1823–1831, 1961.

Cox, D. R., and P. A. W. Lewis, *The Statistical Analysis of Series of Events*, Chapman and Hall, London, 1978.

Eagleson, P. S., *Dynamic Hydrology*, McGraw-Hill, New York, 1970.

Eagleson, P. S., Dynamics of flood frequency, *Water Resour. Res., 8*(4), 878–898, 1972.

Eagleson, P. S., The distribution of catchment coverage by stationary rainstorms, *Water Resour. Res., 20*(5), 581–590, 1984.

Eagleson, P. S., and Q. Wang, The role of uncertain catchment storm size in the moments of peak streamflow, *J. Hydrol., 96*, 329–344, 1987.

Foufoula-Georgiou, E., A probabilistic storm transposition approach for estimating exceedance probabilities of extreme precipitation depths, *Water Resour. Res., 25*(5), 799–815, 1989a.

Foufoula-Georgiou, E., On the accuracy of the maximum recorded depth in extreme rainstorms, in *Proceedings of the IAHS Third Scientific Assembly, 181*, 41–49, Baltimore, M., 1989b.

Fritsch, J. M., R. J. Kane, and C. R. Chelius, The contribution of mesoscale convective weather systems to the warm-season precipitation in the United States, *J. Climate Appl. Meteorol., 25*(10), 1333–1345, 1986.

Gupta, V. K., Transposition of storms for estimating flood probability distributions, *Hydrol. Pap. 59*, Colorado State Univ., Fort Collins, 1972.

Heideman, K. P., and J. M. Fritsch, A quantitative evaluation of the warm-season QPF problem, paper presented at the 10th Conference on Weather Forecasting and Analysis, Am. Meteorol. Soc., Clearwater Beach, Fla, 1984.

Hobbs, P. V., and J. D. Locatelli, Rainbands, precipitation cores and generating cells in a cyclonic storm, *J. Atmos. Sci., 35*(2), 230–241, 1978.

Horton, R. E., Discussion of "The distribution of intense rainfall and some other factors in the design of storm-water drains," by F. A. Marston, *Am. Soc. Civ. Eng., 50*, 660–667, 1924.

Huff, F. A., Time distribution of rainfall in heavy storms, *Water Resour.Res., 3*(4), 1007–1019, 1967.

Huff, F. A., The synoptic environment of flash flood storms, paper presented at the Conference on Flash Floods: Hydrometeorological Aspects, *Am. Meteorol. Soc.*, Los Angeles, 1978.

Huff, F. A., and J. C. Neill, Rainfall relations on small areas in Illinois, *Bull. 44*, Ill. State Water Surv., Urbana, 1957.

Huff, F. A., and R. G. Semonin, An investigation of flood-producing storms in Illinois, *Meteorol. Mono., 4*(22), 50–55, 1960.

Huff, F. A., R. G. Semonin, S. A. Changnon, and D. M. A. Jones, Hydrometeorological analyses of severe rainstorms in Illinois, *Rep. Invest. 35*, Ill. State Water Surv., Urbana, 1958.

Kane, R. J., C. R. Chelius, and J. M. Fritsch, Precipitation characteristics of mesoscale convective weather systems, *J. Clim. Appl. Meteorol., 26*(10), 1345–1357, 1987.

Klemes, V., Empirical and casual models in hydrology, in *Scientific Basis of Water Resource Management, Stud. in Geophys.*, edited by M. B Fiering, pp. 95–104, National Academy Press, Washington, D. C., 1982.

Langbein, W. B., and W. G. Hoyt, *Water Facts for the Nation's Future*, Ronald Press, New York, 1959.

Maddox, R. A., Mesoscale convective complexes, *Bull. Am. Meteorol. Soc., 61*(11), 1374–1387, 1980.

Maddox, R. A., C. F. Chappell, and L. R. Hoxit, Synoptic and meso-β scale aspects of flash flood events, *Bull. Am. Meteorol. Soc., 60*(2), 115–123, 1979.

Maddox, R. A., D. M. Rodgers, and K. W. Howard, Mesoscale convective complexes over the United States during 1981 — Annual summary, *Mon. Weather Rev., 110*(10), 1501–1514, 1982.

Milly, P. C. D., and P. S. Eagleson. Effect of storm scale on surface runoff volume, *Water Resour. Res.. 24*(4), 620–624, 1988.

Rodgers, D. M., K. W. Howard, and E. C. Johnston, Mesoscale convective complexes over the United States during 1982, *Mon. Weather Rev., 111*(12), 2363–2369, 1983.

Rodgers, D. M., M. J. Magnano, and J. H. Arns, Mesoscale convective complexes over the United States during 1983, *Mon. Weather Rev., 113*(5), 888–901, 1985.

Shipe, A. P., and J. T. Riedel, Greatest known areal storm rainfall depths for the contiguous United States, *NOAA Tech. Memo. NWS HYDRO-33*, Office of Hydrol., Natl. Weather Serv., Silver Spring, M., 1976.

U. S. Army Corps of Engineers, *Storm Rainfall in the United States* (ongoing publication of major storm data), Office of the Chief of Eng., Washington, D. C., 1945– .

Veneziano, D., and J. Van Dyck, Statistical analysis of earthquake catalogs for seismic hazard. in *Stochastic Approaches in Earthquake Engineering*, edited by Y. K. Lin and R. Minai, Springer-Verlag, New York, 1987.

Wallace, J. M., and P. V. Hobbs, *Atmospheric Science: An Introductory Survey*, Academic Press. San Diego, Calif., 1977.

Waymire, E., V. K. Gupta, and I. Rodriguez-Iturbe, A spectral theory of rainfall intensity at the meso-β scale, *Water Resour. Res., 20*(10), 1453–1465, 1984.

Wilson, C. B., J. B. Valdes, and I. Rodriguez-Iturbe, On the influence of the spatial distribution of rainfall on storm runoff, *Water Resour. Res., 15*(2), 321–328. 1979.

E. Foufoula-Georgiou, St. Anthony Falls Hydraulic Laboratory, Department of Civil and Mineral Engineering, University of Minnesota, Minneapolis, MN 55414.

L. Wilson, Department of Civil Engineering, FX-10, University of Washington, Seattle, WA 98195.

(Received December 5, 1988;
revised March 13, 1989;
accepted April 19. 1989.)